A R C H I V E S O F M E T A L L U R G Y A N D M A T E R I A L S
Volume 60 2015 Issue 4
DOI: 10.1515/amm-2015-0437

P. ZYGOŃ*,#, M. GWOŹDZIK*, J. PESZKE**, Z. NITKIEWICZ*

# THE EFFECT OF WATER ACRYLATE DISPERSION ON THE PROPERTIES OF POLYMER-CARBON NANOTUBE COMPOSITES

# WPŁYW WODNEJ DYSPERSJI AKRYLANOWEJ NA WŁAŚCIWOŚCI KOMPOZYTÓW POLIMER-NANORURKI WĘGLOWE

The paper presents properties of polymer composites reinforced with carbon nanotubes (CNT) containing various mixtures of dispersion. Acrylates of different particle size and viscosity were used to produce composites. The mechanical strength of composites was determined by three-point bending tests. The roughness parameter of composites was determined with a profilometer and compared with the roughness parameter determined via atomic force microscopy (AFM). Also X-ray studies (phase composition analysis, crystallite sizes determination) were carried out on these composites. Measurements of the surface topography using the Tapping Mode method were performed, acquiring the data on the height and on the phase imaging. The change of intensity, crystallite size and half-value width of main reflections originating from carbon within the composites have been determined using the X-ray analysis. The density of each obtained composite was determined as well as the resistivity at room temperature. The density of composites is quite satisfactory and ranges from 0.27 to 0.35 g/cm$^3$. Different composites vary not only in strength but also in density. Different properties were achieved by the use of various dispersions. Carbon nanotubes constituting the reinforcement for a polymer composite improve the mechanical properties and conductivity composite.

*Keywords*: carbon, nanotubes, AFM, polmer composites, resistivity

W pracy przedstawiono wyniki badań właściwości kompozytów polimerowych wzmacnianych nanorurkami węglowymi zawierających różne dyspersje akrylanowe. Do wytworzenia kompozytów zastosowano akrylany o różnych rozmiarach cząstek i lepkości. Wytrzymałość mechaniczną określono za pomocą próby trójpunktowego zginania. Chropowatość została wyznaczona za pomocą profilometru i porównana z chropowatością wyznaczoną za pomocą mikroskopu sił atomowych (AFM). Na kompozytach przeprowadzono również badania rentgenowskie (analiza fazowa, wielkość krystalitów). Pomiary topografii powierzchni przeprowadzono za pomocą metody Tapping Mode, zbierając dane z wysokości i obrazowania fazowego. Zmiana intensywności, wielkość krystalitów oraz szerokość połówkowa głównego refleksu pochodzącego od węgla została wyznaczona za pomocą analizy rentgenowskiej. W pracy określono również gęstość oraz rezystywność każdego z kompozytów. Gęstość kompozytów jest zadawalająca, gdyż waha się w granicach od 0.27 od 0.35 g/cm$^3$. Kompozyty różnią się zarówno gęstością jak i wytrzymałością a różnice wynikają z zastosowania różnych dyspersji akrylanowej. Nanorurki węglowe dodane do kompozytów poprawiają ich własności wytrzymałościowe oraz przewodność.

## 1. Introduction

Carbon nanotubes were discovered in 1991. They are constructed of a single (single wall carbon nanotubes, SWCNT) or of a few (multiwall carbon nanotubes, MWCNT) concentric and coaxial cylinders, which are rolled single graphene planes [1]. CNTs exhibit excellent mechanical, electrical, thermal and magnetic properties and a significant chemical resistance [2].

Certain types of nanotubes exhibit metallic, while the majority – semiconductor properties. Electric properties are affected by carbon nanotubes diameter and chirality [3, 4].

Thermal and electrical properties, coupled with a high value of Young modulus and tensile strength caused carbon nonotubes to become – relatively quickly – attractive as potential fillers in composite materials [5]. The addition of nanotubes to a polymer matrix can substantially alter the physical properties of the resultant material and make it conductive even at a very limited filler content [6]. An individual approach to the dispersion and the resolution of numerous problems resulting from incompatibilities of carbon nanotubes (CNT) to specific monomers and polymers is required each time to obtain a nanocomposite material with a specific polymer matrix.

* CZESTOCHOWA UNIVERSITY OF TECHNOLOGY, FACULTY OF PRODUCTION ENGINEERING AND MATERIALS TECHNOLOGY, INSTITUTE OF MATERIALS ENGINEERING 19 ARMII KRAJOWEJ AV., 42-201 CZESTOCHOWA, POLAND

** UNIVERSITY OF SILESIA IN KATOWICE , FACULTY OF MATHEMATICS, PHYSICS AND CHEMISTRY, DEPARTMENT OF SOLID STATE PHYSICS, 4 UNIWERSYTECKA STR., 40-007 KATOWICE, POLAND

# Corresponding author: zygon@wip.pcz.pl

One of the most crucial factors in the manufacturing of a nanocomposite material is the provision of suitable dispersion, that is separation of agglomerated CNTs and their homogeneous dispersion in the entire volume of the polymer [7]. Mechanical properties of this material are significantly improved due to a uniform distribution of the reinforcement in the composite matrix.

Carbon nanotubes, when added to polymers, could cause a substantial change of material physical properties, their small amount gives features of a conducting polymer [8]. To achieve the most desired composite physicochemical properties it is important that interaction forces between the dispersed phase and the polymer matrix are as high as possible, the filler distribution in the polymer is homogenous and the filler, is well wettable with polymer [9]. Apart from physico-mechanical properties of the components, the size of the dispersed phase (filler), contact area and the nature of interactions between the continuous and dispersed phase play a significant role in properties of polymer composites as structural materials [10].

## 2. Material and experimental methods

CNT CO. LTD carbon nanotubes, with a commercial name $C_{TUBE\ 100}$, obtained using the thermal CVD method and polyvinyl alcohol with a water acrylate dispersion, were used as the studied materials. As received CNTs were 1 to 25 μm long, 10 to 40 nm in diameter, with the density of 0.03 – 0.06 g/cm$^3$ and the specific surface area of 150 – 250 m$^2$/g. Polyvinyl alcohol (PVA) with a water acrylate dispersion (Osakryl OSA-319M, Oskaryl AZ, Oskaryl OA) was used as the matrix.

Individual dispersions differed in the particle size and viscosity. From the product technical data sheet we have: Osakryl OSA-319M – an average particle size of 120 – 160 nm, viscosity 3000 – 9000 mPa×s; Osakryl AZ – an average particle size has not been specified, viscosity 15-25 mPa×s; Osakryl OA – an average particle size of 150 – 250 nm, viscosity 3000 – 9000 mPa×s. Composites were produced using the solvent method, i.e. via mixing in the solution. Carbon nanotubes used for the reinforcement of composites were not pre-treated or modified. In the first stage both polymers (PVA and an appropriate acrylate) were blended and then carbon nanotubes has been added. The whole was mechanically mixed during 0.5h to disperse well carbon nanotubes in the polymer. After spontaneous evaporation of the solvent, composites were crosslinked at room temperature during 30 days.

Produced composites featured various types of water acrylate dispersion. The composition of produced composites is presented in Table 1.

The test specimens of 10 mm x 10 mm x 60 mm dimensions were cut for three-point bending. Tests were carried out using a ZWICK/ROELL Z100 testing machine with the load cell capacity of 50 kN.

Roughness was measured using a T600 HOMMEL TESTER, in which the surface shape is mechanically scanned by system of moving inductive converter. Studies of surface topography were performed using a VEECO MULTIMODE atomic forces microscope (AFM) with a NANOSCOPE controller by means of the Tapping Mode method. The surface studies were carried out in the area of 5 mm x 5 mm.

The X-ray phase analysis was carried out using a SEIFERT 3003T/T X-ray diffractometer with the following parameters: measurement step 0.1°, integration time 3 seconds, characteristic radiation wavelength $\lambda_{Co}$=0.17902 nm. To interpret the results (to determine the 2θ position and the total intensity $I_{Net}$ and the crystallite sizes) the diffractograms were described by a Pseudo Voight curve using the Analyze software.

TABLE 1

Composition of produced composites [% wt.]

| | CNT [%] | PVA [%] | Water acrylate dispersion Osakryl | | |
|---|---|---|---|---|---|
| | | | OSA 319M [%] | AZ [%] | OA [%] |
| **Composite 1** | 12 | 70 | 18 | - | - |
| **Composite 2** | 12 | 70 | - | 18 | - |
| **Composite 3** | 12 | 70 | - | - | 18 |

The density of each composite was also measured. The method of density measurement consists of independent measurement of specimen's mass and volume. The mass of specimens was determined by means of an electronic balance (Δ±0.01 g) and the volume of cuboidal specimens via measuring their dimensions using a vernier caliper (Δ±0.01mm).

The measurements of the electric resistivity have been performed on the stand, schematically presented in Fig. 1, equipped with a Keithley 6417B electrometer, which enables exact measurements of surface current Is, as well as with certified measurement electrodes. The samples were conditioned for 24 hours at the temperature of 22.5°C and relative humidity of 65%.

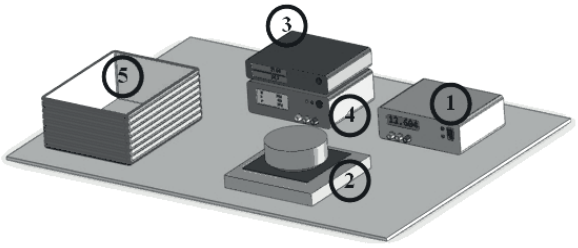


Fig. 1. The diagram of the stand for measurements of static charge and surface resistivity [developed by Adam Jakubas]: 1 – programmable electrometer, 2 – set of shielded ring-shaped electrodes, 3 – device for humidity and temperature measurements, 4 – stabilised power supply 0÷400 V, 5 – chamber for sample conditioning

## 3. Results of tests

Composite roughness measurements were performed on LT = 4.80 mm long with the precision of LC = 0.80 mm. Each specimen was scanned five times. Tests resulted in graphs, where voltage changes were recorded in the form of peaks, evaluated by means of the instrument head electronics, which are converted into a signal proportional to position changes of the diamond tip, by means of which appropriate surface parameters are displayed and documented.

Basic parameters of studied material surface roughness include:
- $R_a$ – arithmetical mean roughness deviation,
- $R_{max}$ – maximum roughness height,
- $R_t$ – maximum elevation – cavity height,
- $R_z$ – average roughness height,
- $R_p$ – maximum height of elevation.

The roughness results obtained (Tab. 2) demonstrated that composite material 1 (OSA-319M) attained the highest roughness value. The standard deviation is Δ±47 nm. On the other hand, the matrix itself demonstrated the lowest roughness values.

From the roughness diagrams obtained (Fig. 2) one can be noticed high peaks, which indicate a high roughness of the composite material surface. The highest roughness has been observed for composite material 1 (OSA-319M), for which the average roughness parameter amounted to ~17 μm. The lowest value of roughness parameter has been observed in the case of matrix, for which that parameter had the value of ~1μm.

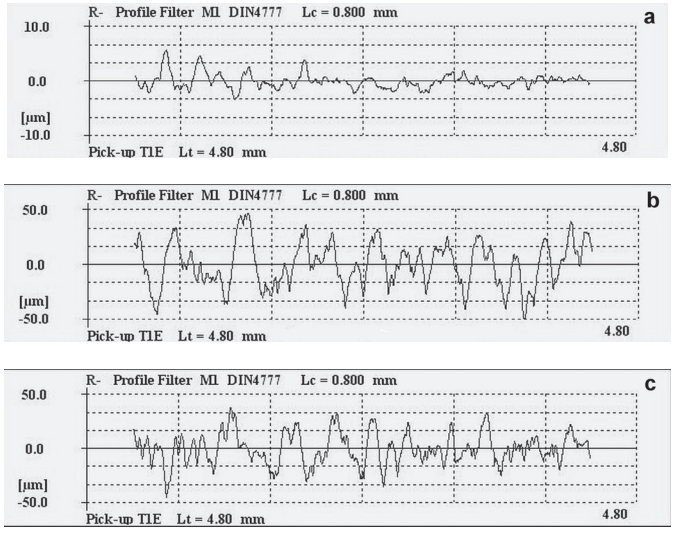


Fig. 2. Roughness profiles for individual composite and the matrix: a) matrix; b) composite 1 (OSA-319M); c) composite 2 (AZ); c) composite 3 (OA)

Figure 3-5 shows the 3D image and topography of investigated composites materials. Figure 3a presents the 3D image of surface topography of composite material 1 (OSA-319M), obtained during the examination using an atomic force microscope.

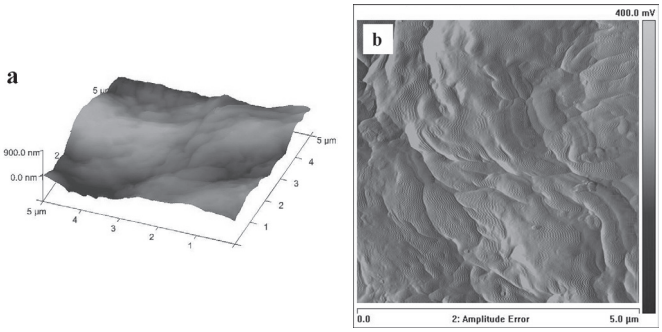


Fig. 3. Surface topography of composite material 1 (OSA-319M): a) 3D surface topography; b) amplitude of vibrations

It can be noticed there characteristic strips resulting from the arrangement of nanotubes. The distribution of carbon nanotubes in the composite material can be seen clearly in Fig. 3b, which show the amplitude image.

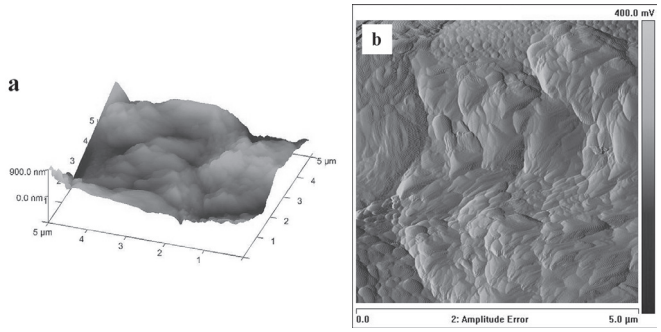


Fig. 4. Surface topography of composite material 2 (AZ): a) surface topography 3D; b) amplitude of vibrations

Figure 4 presents the image of composite material 2 (Osakryl AZ). In that composite material, a fairly chaotic distribution of nanotubes in the matrix of the composite material can be seen. It can be noticed, however, that some nanotubes have been well separated in the process of composite material processing.

TABLE 2

Basic roughness parameters of studied composites surface

| | Matrix (OSA-319M) | Composite 1 (OSA-319M) | Composite 2 (AZ) | Composite 3 ( OA) |
|---|---|---|---|---|
| Ra [μm] | 0.97 | 16.72 | 11.19 | 10.93 |
| Rmax [μm] | 7.96 | 88.86 | 70.18 | 79.67 |
| Rt [μm] | 9.19 | 96.27 | 83.78 | 88.55 |
| Rz [μm] | 5.08 | 78.60 | 62.07 | 58.38 |
| Rp [μm] | 5.76 | 46.69 | 38.01 | 32.06 |

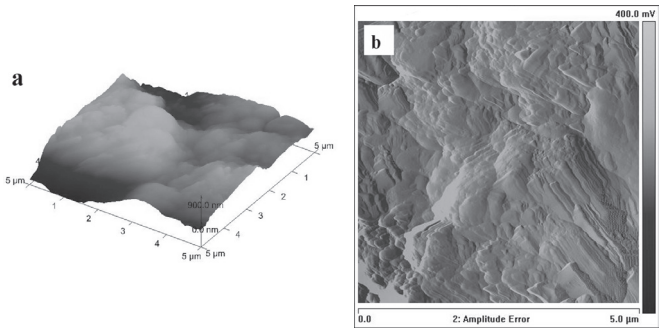


Fig. 5. Surface topography of composite material 3 (OA): a) surface topography 3D; b) amplitude of vibrations

Figure 5 presents the topography of surface of composite material 3 (Osakryl OA). Clusters of nanotubes that have not been dispersed are visible, although they are not very large.

Measurements of surface topography and vibrations amplitude for the matrix have also been carried out. The results of those examinations are presented in Figure 6.

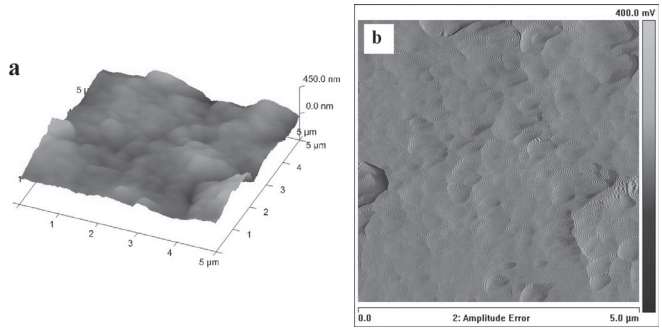


Fig. 6. Surface topography of matrix: a) surface topography 3D; b) amplitude of vibrations

Roughness parameters $R_a$ and $R_{max}$ (Fig. 7) were determined from the surface of the composites and the surface of matrix. Also the standard deviation was calculated, which is equal Δ±2.1 nm.

The lowest value of roughness parameter was demonstrated by the matrix, for which the average roughness parameter $R_a$ amounted to ~35nm, while the maximum roughness value was ~373 nm. Composite materials are characterised by a similar roughness, which varies from 108 to 136 nm (Fig. 7).

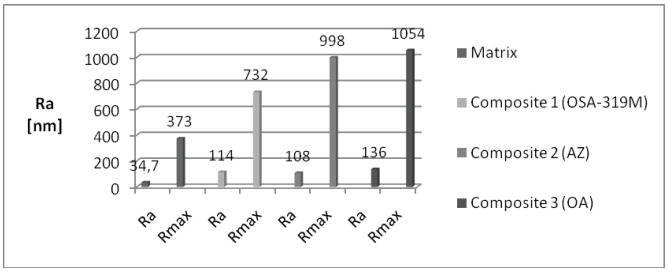


Fig. 7. Avarage arithmetical roughness for individual composites, Δ±2.1 nm

The results of X-ray investigation are presented in Fig. 8. The X-ray phase analysis has shown that characteristic reflections originating from carbon are visible on the all diffractograms.

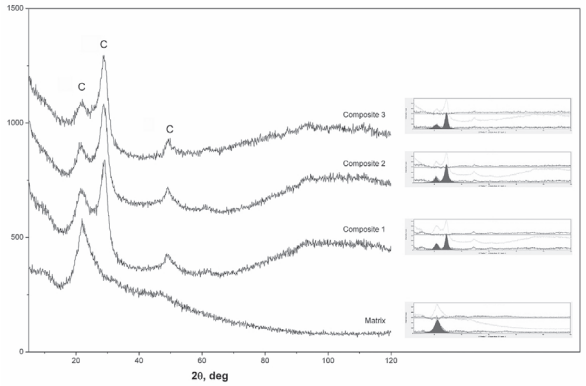


Fig. 8. The X-ray diffractograms of individual composites with fitting by means of the Analyze software

The peak characteristic of the matrix originates from carbon in the hydrocarbon chain, which is typical of polymers. The hybridisation that occurs between such atoms of carbon is $sp^3$. On the other hand, the peaks that are visible on diffractograms of composite materials originate from graphite. For such connections between carbon atoms the $sp^2$ hybridisation is characteristic.

Main reflections from carbon in the hydrocarbon chain and from graphite in carbon nanotubes were analysed more thoroughly. The total intensity of reflections originating from carbon as well as from graphite turned out to be the highest for composite material 1 (OSA-319M), and the lowest for composite material 3 (OA) (Fig. 9). On the other hand, the total intensity originating from carbon is much higher for the matrix than for composite materials.

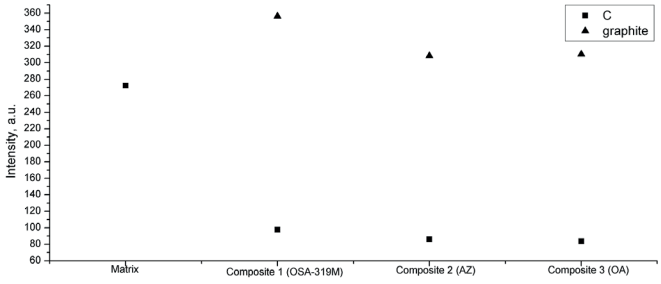


Fig. 9. Total intensity of the main reflection originating from carbon

The narrowest diffraction line has been observed for composite material 1 (OSA-319M) (Fig. 10), whereas the widest one for composite material 2 (AZ), which is caused by reduction of crystallite size (Fig. 11).

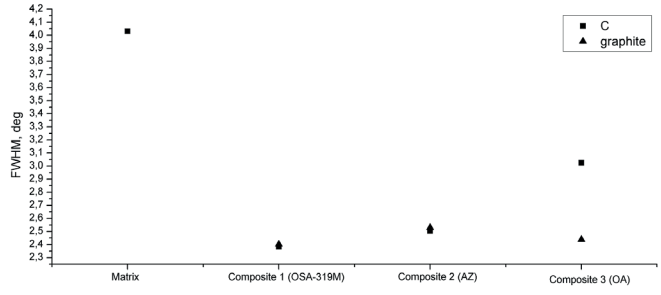


Fig. 10. Half-value width of the main reflection originating from carbon

X-ray examinations performed on composite materials have revealed that not only the intensity of reflections changes, but also their full width at half maximum (FWHM). As it is known, the change in width may result both from a change in the size of crystallites, as well as from residual stresses in the material. Composite material 1 (OSA-319M) is characterised by having biggest crystallites (Fig. 11) derived both from carbon and graphite, that varies for composite materials 2 (AZ) and 3 (OA). On the other hand, the lowest carbon-derived crystallite size has been observed for the matrix.

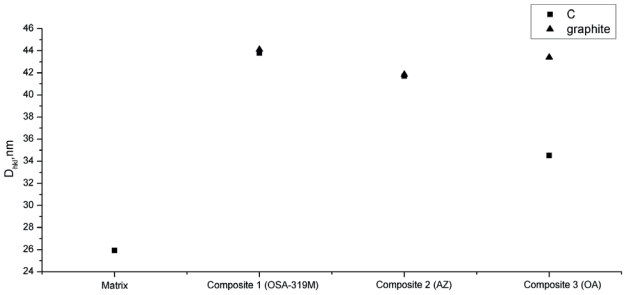


Fig. 11. $D_{hkl}$ crystallite sizes for the main reflection originating from carbon

The results of resistivity measurements, flexural strength, and density of the different composite materials are summarized in Table 3.

TABLE 3
The results of bending strength, density and resistivity for individual composites

| | Denisty d [g/dm3] | Resistivity ρs [Ω×m] | Bending strength Rg [MPa] |
|---|---|---|---|
| Composite 1 (OSA-319M) | 0.35 | 372 | 4.054 |
| Composite 2 (AZ) | 0.27 | 107 | 0.721 |
| Composite 3 (OA) | 0.31 | 676 | 1.181 |
| Matrix | 1.22 | 2.84×1010 | - |

The highest resistivity and density have been observed for the composite material containing Osakryl OA dispersion. Its resistivity was found to be 676 Ω×m. The lowest resistivity was attained by the composite material containing Osakryl AZ dispersion – 107 Ω×m.

Figure 12 shows flexural strength of the composite materials.

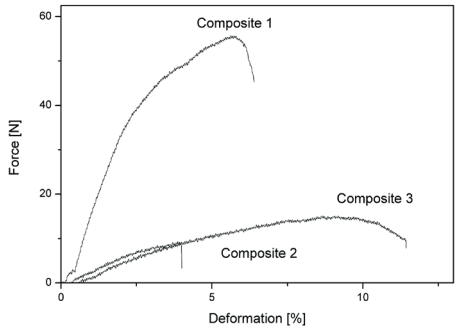


Fig. 12. Force vs. deformation for the three-point bending test for the composites

Graphs provide information about the maximum force used to break a sample, on that basis the flexural strength has been determined (Table. 3). The highest value of flexural strength has been observed for composite material 1 (OSA-319M), for which the Rg value amounted to 4.054 MPa. For composite material 3 (OA) the flexural strength amounted to 1.181 MPa, whereas composite material 2 (OZ) revealed the lowest flexural strength. For the latter, the value of Rg was 0.721 MPa.

## 4. Summary of results

The paper presents possibilities of nanocomposite materials production. The most important thing for each engineer is to produce materials of as good as possible mechanical properties.

It can be concluded from the studies of surface topography, conducted on a profile measuring device, that the highest level of roughness occurs for composite material 1 (OSA-319M), for which the value of Ra is ~17 mm. Composite materials 2 (AZ) and 3 (OA) have a similar roughness parameter, about ~11 mm. The lowest value of roughness parameter was observed for the matrix, for which that parameter had the value of ~1μm. The results of profilometry confirmed the results of roughness measurements performed using AFM. The examinations of surface topography, performed by means of the atomic force microscopy (AFM), revealed that all composite materials have similar roughness values, which were within the 700 nm – 1 mm range. On the other hand, the matrix is characterised by significantly lower Ra coefficient, amounting to 35 nm.

It was observed from the X-ray examinations that the characteristic peak, which has been noted for composite materials is a graphite-derived peak. Also the carbon-derived peak, typical for hydrocarbon chains, was visible. The size of crystallites derived from carbon was the largest for composite material 3 (OA), and the lowest for the matrix, which translates into full width at half maximum, which is the largest for the matrix and the smallest for composite material 3 (OA). For the other composite materials both the full width at half maximum, intensity, and size of the crystallite were identical.

The density of composite materials varies in the range of 0.27 – 0.25 g/cm$^3$.

The highest strength parameter has been observed for composite material 1 (OSA-319M), for which Rg amounted to 4.054 MPa, whereas the lowest flexural strength has been noted for composite material 2 (AZ). For the latter, the Rg amounted to 0.721 MPa.

Addition of nanotubes to the matrix yielded a remarkable improvement to the conductivity of composite materials. The resistivity for the matrix alone amounted to $2.84\times10^{10}$ Ω×m, whereas after the addition of nanotubes it varied from 107 to 676 Ω×m. Carbon nanotubes significantly improved the conductivity of composite materials.

The studies conducted show that the best properties have been achieved for composite material 1, which contains OSA-319M dispersion. OSA-319M acrylate dispersion has turned out to be the best additive to such composites due to its finest particles and the highest viscosity.

Effective and affordable production and stabilisation

methods should be developed for nanomaterials, so that they could be more often used in practice. Not only the strength characteristic of nanocomposites but also its skilful use in a composite material decide about their practical application possibilities.

## REFERENCES


[1] S. Ijima, Helical microtubules of graphitic carbon, Nature **54**, 56 – 58 (2001)

[2] P. Zygoń, M. Gwoździk, J. Peszke, Z. Nitkiewicz, Surface topography of carbon nanotubes posing a reinforcing phase in composite materials, Kompozyty **4**, 262-265 (2012)

[3] A. Huczko, Nanorurki węglowe, Czarne diamenty XXI wieku, Warszawa 2004

[4] P. Zygoń, J. Peszke, M. Gwoździk, Z. Nitkiewicz, M. Malik, Characteristic of Carbon Nanotubes Modified with Cobalt, Copper and Bromine, Archives of Metallurgy and Materials **59**, 2, 675-679 (2014)

[5] M. S. Dresselhaus, G. Dresselhaus, Ph. Avouris, Carbon nanotubes, Advanced Topics in the Synthesis, Structure, Properties and Applications, Topics Appl. Phys. **80**, 1–9, 2001

[6] J. K. W. Sandler, J. E. Kirk, I.A. Kinloch, M. S. P. Shaffer, A. H. Windle, Ultra-low electrical percolation threshold in carbon-nanotube-epoxy composites, Polymer **44**, 5893-5899 (2003)

[7] J. Gou, B. Minaie, B. Wang, Z. Liang, C. Zhang, Computational and Experimental. Study of Interfacial Bonding of Single-walled Nanotube Reinforced Composites. Comp. Mat. Sc. **31**, 3-4, 225–236 (2004)

[8] M. Kwiatkowska, G. Broza, J. Męcfel, T. Sterzyński, Z. Rosłaniec, Otrzymywanie i charakterystyka nanokompozytów polimerowych PBT/nanorurki węglowe, Kompozyty **2**, 99-104 (2005)

[9] R. A. Vaia, H. D. Wagner, Framework for nanocomposites. Mater. Today **7**, 11, 32–37 (2004)

[10] Z. Rosłaniec, Nanorurki węglowe i Nanokompozyty polimerowe z ich udziałem, Zeszyty Naukowe Politechniki Poznańskiej 4, 211-215 (2007)


*Received: 15 September 2014..*